APPLIED ORGANOMETALLIC CHEMISTRY
Appl. Organometal. Chem. 2005; **19**: 81–89
Published online in Wiley InterScience (www.interscience.wiley.com). DOI:10.1002/aoc.838

Evidence of colloidal rhodium formation during the biphasic hydroformylation of 1-octene with thermoregulated phase-transfer phosphine rhodium(I) catalyst

Fei Wen[1,2], Helmut Bönnemann[1]*, Jingyang Jiang[2], Dongmei Lu[2], Yanhua Wang[2] and Zilin Jin[2]

[1]Max-Planck-Institut für Kohlenforschung, Kaiser-Wilhelm-Platz 1, D-45470 Mülheim an der Ruhr, Germany
[2]State Key Laboratory of Fine Chemicals, Dalian University of Technology, 116012 Dalian, P.R. China

Received 31 August 2004; Revised 16 September 2004; Accepted 23 September 2004

A thermoregulated phase-transfer (TRPT) Rh(I) complex catalyst A prepared from $Rh(acac)(CO)_2$ and a thermoregulated ligand $CH_3(OCH_2CH_2)_mPPh_2$ ($M_w = 918$) was applied to the biphasic hydroformylation of 1-octene, and a high activity with an aldehyde yield of 97.5% was demonstrated. After three recycling steps, the aldehyde yield gradually decreased. Transmission electron microscopy (TEM) revealed that after the first cycle Rh colloids were generated *in situ* in the aqueous phase, and in subsequent runs Ostwald ripening occurred. An independently prepared colloidal Rh(0) TRPT catalyst D also exhibited high hydroformylation activity under identical experimental conditions, and after two times of recycling an activity decrease was also observed. It is suggested that *in situ* from $Rh(acac)(CO)_2$ colloidal Rh particles are generated, which demonstrate thermomorphic behaviour and a high hydroformylation activity. Subsequently, agglomeration processes result in an activity decay, as observed in the TRPT Rh(I) complex catalyst system. Copyright © 2004 John Wiley & Sons, Ltd.

KEYWORDS: thermoregulated phase-transfer catalysis; rhodium colloid catalyst; biphasic hydroformylation

INTRODUCTION

The catalytic behaviour of transition-metal colloids has been a very active research field in past decades due to their structural characteristics, which are expected to combine the advantages of both heterogeneous and homogeneous catalysis, i.e. a 'heterogeneous catalysis in solution'.[1] Metal colloids may serve as a medium to investigate the relationship between heterogeneous and homogeneous catalytic mechanisms. Various transition-metal colloids stabilized by surfactants or solvents have been applied to hydrogenation,[2–6] oxidation,[7–10] hydrosilylation[11–14] and C–C coupling reactions.[15,16] On the other hand, *in situ*-generated metal colloids have been observed during homogeneous catalytic reactions using transition-metal complexes.[17] Very recently, studies focusing on the function of these *in situ*-generated colloids have attracted increasing attention.[14,17–23]

The aqueous biphasic hydroformylation of propene, namely the Ruhrchemie/Rhône-Poulenc (RCH/RP) process, was industrialized by Ruhrchemie in 1984 and has been used widely to produce *n*-butanal because the water-soluble catalysts can be separated easily and completely from the water-insoluble products.[24] However, the rate of hydroformylation drops dramatically with increasing alkyl chain length of olefins ($>C_5$) because of their poor solubility in water.[25] A variety of tentative approaches have been proposed to overcome this problem.[26] Jin *et al.* developed a concept of 'thermoregulated phase transfer catalysis (TRPTC)', i.e. at higher temperatures the water-soluble catalyst migrates into the organic phase to catalyse the reaction, and at lower temperatures returns to the aqueous phase. Therefore, by using biphasic systems the catalyst-containing phase can be recovered easily by decantation, and extremely water-immiscible substrates can be hydroformylated.[27,28]

*Correspondence to: Helmut Bönnemann, Max-Planck-Institut für Kohlenforschung, Kaiser-Wilhelm-Platz 1, D-45470 Mülheim an der Ruhr, Germany.
E-mail: boennemann@mpi-muelheim.mpg.de

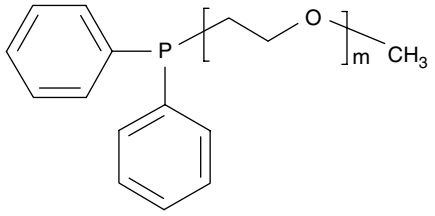

Scheme 1. Ligand **a** ($M_w = 918$).

Based on this concept, a series of phosphine ligands with distinct cloud points having an inversely temperature-dependent solubility in water have been prepared and were applied successfully to the aqueous biphasic hydroformylation of long-chain alkenes.[29–31] Typical TRPT catalysts can be recovered and reused efficiently, although in most cases the activity decays after several recycling steps. Because the reaction was performed under a reductive atmosphere (CO/H_2), and colouration of the aqueous catalyst phase was generally observed during the hydroformylation, we examined the catalyst phase by transmission electron microscopy (TEM) to check whether Rh colloids were generated *in situ* during the catalytic reaction. Although it is generally accepted that the formation of metallic precipitates causes decomposition of the homogeneous Rh catalyst, no detailed study on the intermediate role of colloidal Rh particles in hydroformylation reactions was available.

In this study, biphasic hydroformylation of 1-octene was performed with TRPT Rh(I) complex catalyst **A**, using $Rh(acac)(CO)_2$ as the catalyst precursor and a novel thermoregulated phosphine $CH_3(OCH_2CH_2)_mPPh_2$ ($M_w = 918$), **a**, as the ligand (Scheme 1). Rhodium colloids both in water-soluble form (hydrosol)[32] and in organic solution (organosol)[33] were prepared via Bönnemann's methods. Both colloid types were dispersed in the aqueous phase by ligand **a**, and applied to the hydroformylation of 1-octene under identical experimental conditions. This enabled us to examine the contribution of *in situ*-formed Rh colloids to the hydroformylation reaction and to check the activities of pre-prepared TRPT colloidal Rh catalysts for the biphasic hydroformylation of long-chain alkenes.

EXPERIMENTAL

Compounds $Rh(acac)(CO)_2$, anhydrous $RhCl_3$, tri(*m*-sulphonyl)triphenylphosphine trisodium salt (TPPTS) and *n*-dodecyl-*N*,*N*-dimethy-3-ammonio-1-propanesulphonate (Sulfobetaine 12, SB12) are commercially available. Ligand **a** was prepared from $CH_3OPEG_{750}OS(O)_2CH_3$ and $LiPPh_2$ according to literature.[63]

All reactions and operations were performed under argon using standard Schlenk and syringe techniques, unless stated otherwise. Organic solvents were carefully dried and saturated with argon. 1-Octene, *n*-pentane and *n*-decane were redistilled and saturated with argon prior to use. For the hydroformylation reactions, deoxygenated water was used.

Preparation of complex catalyst A: $Rh(acac)(CO)_2$/ligand a

Catalyst precursor $Rh(acac)(CO)_2$ (30 mg, 0.116 mmol) was introduced into a solution of ligand **a** (0.53 mg, 0.58 mmol) in CH_2Cl_2 (30 ml) according to a ratio of [P]/[Rh] = 5. The resulting mixture was stirred at 25 °C for 1 day. Then the solvent was evaporated out under reduced pressure and 32 ml of water was added. The resulting yellow solution **A** was ready for use.

Preparation of Rh colloid 1 (hydrosol)[32]

To a stirred suspension of SB12 (9.86 g, 29.4 mmol) in tetrahydrofuran) (THF, 300 ml) was added dropwise a solution of lithium triethylborohydride ($Li[BEt_3H]$, 3.25 g, 30.78 mmol) in THF (19 ml). The resulting clear solution was added dropwise to a suspension of anhydrous $RhCl_3$ (2.05 g, 9.7 mmol) in THF (300 ml) at 65 °C over 28 h. The resulting black mixture was stirred at 65 °C for a further 2 h and then cooled down to room temperature. After addition of 10 ml of acetone, the reaction mixture was allowed to settle for 16 h. Following removal of the clear supernatant, the black–brown precipitates were washed by another 10 ml of acetone. After concentration and drying under vacuum, the residue was dissolved in 14 ml of water, and addition of 30 ml of acetonitrile caused the formation of a dark greyish-brown precipitate. The mixture was allowed to settle for 16 h and then heated to 80 °C for 10 min. Finally, the clear supernatant solution was removed, and further drying under vacuum yielded a grey colloidal powder (3.98 g) (**1**, Scheme 2) which proved to be very soluble in water and ethanol. Elemental analysis: Rh, 23.90%. Particle size (TEM): 2.6 ± 0.6 nm.

Preparation of colloidal catalyst B: Rh colloid 1/ligand a

Rhodium colloidal powder **1** (31 mg, 0.072 mmol) was introduced into 20 ml of an aqueous solution of ligand **a** (0.33 g, 0.36 mmol) according to a ratio of [P]/[Rh] = 5, and stirred at 25 °C for 1 day. The resulting yellow solution **B** was ready for use.

Preparation of complex catalyst C: $Rh(acac)(CO)_2$/TPPTS

Catalyst precursor $Rh(acac)(CO)_2$ (30 mg, 0.116 mmol) was introduced into 32 ml of an aqueous solution of TPPTS (329 mg, 0.58 mmol) according to a ratio of [P]/[Rh] = 5, and stirred at 25 °C for 1 day. The resulting yellow solution **C** was ready for use.

Preparation of Rh colloid 2 (organosol)[33]

A solution of tetraoctylammonium triethylhydroborate, $N(octyl)_4[BEt_3H]$, in THF (210 ml, 0.19 M) was added dropwise at 40 °C over 1 h to a suspension of anhydrous $RhCl_3$ (2.79 g, 13.33 mmol) in THF (390 ml). Stirring at 40 °C

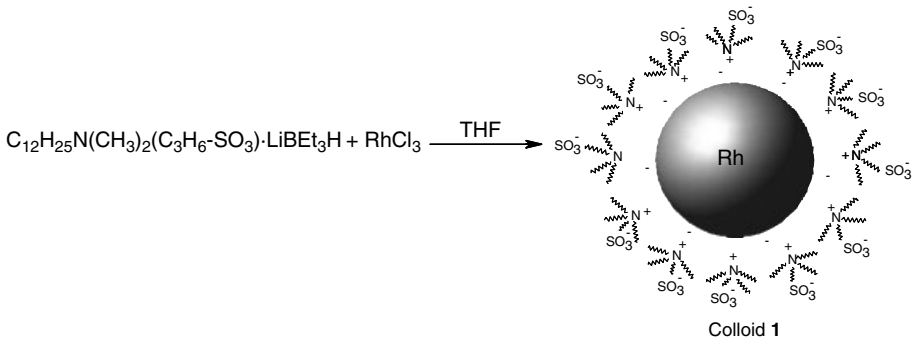

Scheme 2.

for 3 h and then at 25 °C for 15 h gave a black solution. After filtration, the clear, dark-black solution was concentrated and dried under vacuum. The black–brown waxy residue was redissolved in 500 ml of technical quality ether without protective gas, and further addition of 50 ml of technical quality ethanol caused a grey–black precipitate. After removing the clear supernatant, the precipitate was washed again with a mixture of ether (100 ml) and ethanol (10 ml). Following removal of the supernatant, drying under vacuum gave 1.1 g of black Rh colloidal powder (**2**, Scheme 3), which was soluble in THF and partially soluble in toluene. Elemental analysis: Rh, 80.21%. Particle size (TEM): 1.9 ± 0.4 nm.

Preparation of colloidal catalyst D: Rh colloid 2/ligand a

Rhodium colloidal powder **2** (20 mg, 0.16 mmol) was added to a biphasic system of 30 ml of toluene and 30 ml of H_2O. After shaking, the toluene layer gave a black colour due to the dissolution of rhodium colloid, whereas the water layer remained colourless. Then, 740 mg of ligand **a** (0.80 mmol) was added to the biphasic system and the mixture was stirred at 25 °C for 1 day. After settling for another day, the organic layer turned colourless and the aqueous layer became black–brown. The upper toluene layer was removed and the aqueous phase was washed twice with 10 ml of fresh toluene. Finally, the aqueous phase was diluted with 14 ml of water to obtain a colloidal aqueous solution **D**, which was ready for catalytic reaction. The catalyst could be obtained also in a black waxy form after evaporation and drying under vacuum; this form was soluble in water, partially soluble in ethanol and ether and slightly soluble in THF and $CHCl_3$.

Hydroformylation

Hydroformylation reactions were carried out in a 50-ml stainless-steel autoclave equipped with a magnetic stirrer. All preformed catalyst solutions were diluted to [Rh] = 3.6 mM and [P] = 18 mM with a ratio of [P]/[Rh] = 5. A typical experiment was performed in the following manner (Table 1, entry 1). The Rh(I) catalyst aqueous solution **A** and a mixture of 1-octene, *n*-pentane and *n*-decane (internal standard) were transferred to the evacuated autoclave by syringe. Then the autoclave was pressurized up to 40 bar of syngas and heated to 90 °C under stirring. The reaction was kept at 90 °C for 4 h. After cooling down and depressurizing, the upper organic layer was decanted and analysed by gas chromatography–mass spectrometry (GC–MS). Then a fresh batch of 1-octene, *n*-pentane and *n*-decane were introduced to perform the next cycle.

Mercury poisoning test

A mercury poisoning test was performed when using colloidal catalyst **D** in the hydroformylation reaction. After six cycles, the organic product layer was removed from the autoclave and 1.5 g of Hg(0) (350 equiv. of Rh) together with a fresh batch of 1-octene, *n*-pentane and *n*-decane were added. The reaction mixture was stirred at 25 °C for 1 h and then pressurized up to 40 bar of syngas and heated to 90 °C under

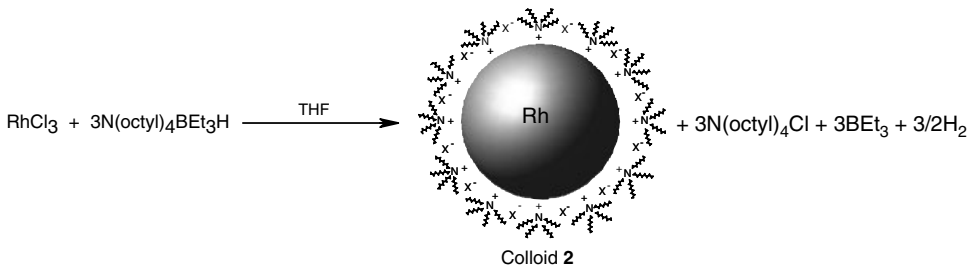

Scheme 3.

Table 1. Hydroformylation[a] of 1-octene with complex catalyst **A** in the aqueous biphasic system

Entry	Cycle	Conversion (%)	S_{ald}[b] (%)	L/B ratio	S_{iso}[b] (%)
1[c]	1	98.3	97.5	2.4	0.8
	2	98.1	96.8	2.4	1.3
	3	99.7	97.3	2.4	2.4
	4	99.0	94.5	2.4	4.5
	5	98.1	91.8	2.4	6.3
	6	99.9	89.7	2.2	10.2
	7	98.0	75.6	1.9	22.3
	8	97.3	68.3	1.8	29.0
2[d]	1	99.2	96.7	2.1	2.5
3[e]	1	99.6	78.8	2.0	20.8

[a] Reaction conditions: $P_{initial} = 40$ bar (25 °C), $CO/H_2 = 1:1$, $T = 90$ °C, $t = 4$ h, $V_{organic}/V_{aqueous} = 1.5$, [P]/[Rh] = 5.
[b] S_{ald}, selectivity in aldehydes; S_{iso}, selectivity in isomeric octenes (2- and 3-octene).
[c] [Rh] = 3.6 mM, ratio of 1-octene to catalyst ([Sub]/[Rh]) = 1000.
[d] [Rh] = 1.8 mM, [Sub]/[Rh] = 2000.
[e] [Rh] = 0.9 mM, [Sub]/[Rh] = 4000.

stirring. The reaction was kept at 90 °C for 4 h, as with the previous cycles.

Characterization

^1H, ^{13}C and ^{31}P NMR measurements were carried out on a Bruker DPX-300 spectrometer to check the feasibility of the ligand exchange process for the preparation of TRPT colloidal catalyst **D**. Chemical shifts of ^1H and ^{13}C NMR spectra were calibrated according to the deuterated solvent signals and converted to the $Si(CH_3)_4$ scale. The ^{31}P NMR spectra were recorded with 85% H_3PO_4 as an external reference.

Gas chromatography–mass spectrometry experiments were carried out with an HP 5890 gas chromatograph coupled to a Finnigan SSQ 7000 quadrupole mass spectrometer to determine the conversion and selectivity of the hydroformylation reactions. Separations were accomplished on an RTX-1 capillary column (30 m × 0.25 mm I.D., film thickness 0.25 μm).

Transmission electron microscopy (TEM) measurements were performed using a Hitachi H 7500 instrument operated at an accelerating voltage of 120 kV. Specimens were prepared by placing a drop of the post-reaction aqueous phase on a carbon film, which was supported on a copper grid, and then drying at room temperature. Energy-dispersive X-ray spectroscopy (EDX) analyses were performed to obtain a chemical analysis of the colloid particles using an Oxford Instruments INCA EDX spectrometer attached to the microscope.

Ultraviolet–visible (UV–Vis) spectroscopy analyses were performed on a Varian Cary 500 UV spectrophotometer.

Inductively coupled plasma optical emission spectroscopy (ICP-OES) analyses were carried out on an Iris Interpid DUO ER/S instrument (Thermo Elemental, USA) to check the amount of leaching Rh in the organic layers.

Elemental analyses of Rh colloids **1** and **2** were performed at H. Kolbe Microanalysis Laboratory, Muelheim an der Ruhr, Germany.

RESULTS AND DISCUSSION

Complex catalyst A: Rh(I)/ligand a

First, we studied the biphasic hydroformylation of 1-octene with TRPT complex catalyst **A**, using $Rh(acac)(CO)_2$ as the precursor and **a** as the ligand. The hydroformylation reaction was performed at 90 °C, just above the cloud point of ligand **a** (85 °C). As shown in Table 1 (entry 1), catalyst **A** provides a very high hydroformylation activity towards 1-octene. The aldehydes are produced in 97.5% yield and a linear to branched (L/B) ratio of 2.4, but no hydrogenation products are observed.

Then the recycling was evaluated. Table 1 (entry 1) shows that after five cycles the aldehyde yield is still as high as 91.8% and selectivity of the linear aldehyde is maintained. The high activity and recyclability of catalyst **A** correspond to the thermomorphic behaviour of TRPT catalysts in aqueous biphasic reaction, i.e. the hydroformylation of 1-octene takes place in the organic phase. In addition, Table 1 mirrors the gradually increasing isomerization rate from 1-octene to internal octenes (2-octene and 3-octene) with increasing number of runs, which may correspond to the decreasing aldehyde yield, considering the very low hydroformylation rate of internal alkenes.

During the reaction, it was observed that the aqueous phase turned from light yellow to dark brown after the first cycle. Because the colouration in homogeneous catalysis generally arises from colloidal metal formation,[14,34] in the present study the aqueous layers after reaction were examined by TEM and UV–Vis spectroscopy. As shown in Fig. 1a, colloidal particles of 2.2 ± 0.5 nm are observed after the first run. Figure 1b indicates that the colloidal size increases to 2.6 ± 0.4 nm after the second run, and Fig. 1c shows that agglomeration starts after the third run resulting in a mean diameter at 3.0 nm. A severe agglomeration takes place after five cycles (Fig. 1d). After the seventh cycle, only very small colloidal particles of 1.5 ± 0.3 nm are left in solution. Finally, after recycling, Rh black was observed in the autoclave. Energy-dispersive X-ray spectroscopy revealed that the particles observed in TEM were colloidal Rh.

Herein, the behaviour of *in situ*-generated colloids can be ascribed to an Ostwald ripening process, which introduced two limiting mechanisms for cluster growth: the first involved diffusion of intact clusters and subsequent coalescence of the diffusing clusters; the second involved detachment of atoms from smaller clusters and then reattachment to larger clusters.[35–38] Hence, the colloids generated during the hydroformylation reaction were comparatively stable in the first two cycles and then started to aggregate. These Rh aggregates precipitated out later when Rh black was observed after the reaction. Therefore, only small-sized

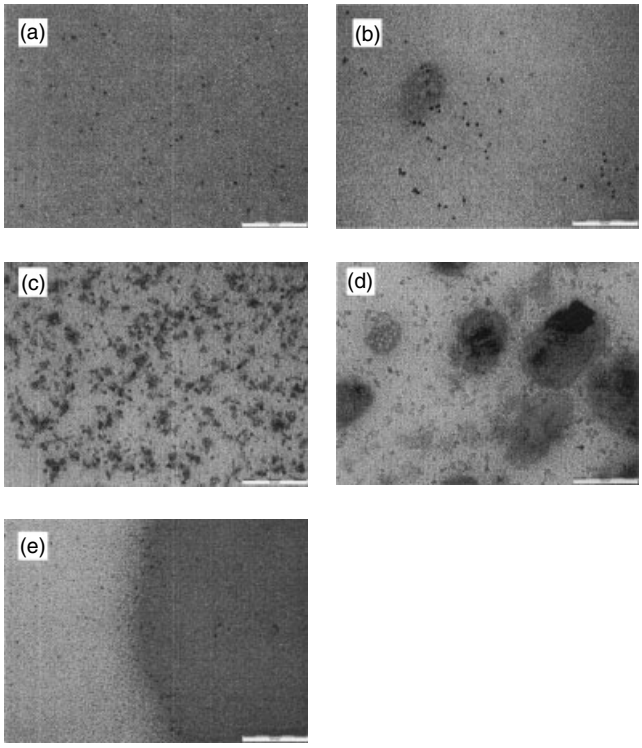

Figure 1. Transmission electron micrographs of the post-reaction aqueous phase when using complex catalyst **A**: (a) first run (2.2 ± 0.5 nm); (b) second run (2.6 ± 0.4 nm); (c) third run (3.0 ± 0.8 nm); (d) fifth run (4.2 ± 1.3 nm; larger ones: 40–60 nm); (e) seventh run (1.5 ± 0.3 nm). Scale bar: 50 nm.

colloidal particles are left in the post-cycles, as shown in Fig. 1e. Very recently, EI-Sayed *et al.*[35] attributed the size variations of PVP–palladium nanoparticles observed during the Suzuki reaction to Ostwald ripening. They found that the Pd colloidal particle size increased in the beginning of the reaction and levelled off towards the end of the first cycle, whereas the size decreased when the catalyst was applied to the second cycle, which was explained by the larger nanoparticles aggregating and precipitating from solution. Herein, the Ostwald ripening process seems much slower.

The variations of complex catalyst **A** before and after hydroformylation reaction in entry 1 are also evidenced by UV–Vis spectroscopy (Fig. 2a–d), in which the broad absorption peak at 240–300 nm from Rh(I) gradually decreases with the developing runs, whereas a broad tailing absorption in the range from the ultraviolet to the visible region appears, which may arise from the plasmon resonance of Rh colloids.[39] Prior to hydroformylation, complex catalyst **A** shows a band at 395 nm due to the metal-to-ligand charge transfer transition of Rh(I) to ligand **a**, which becomes obscure after the first cycle and almost disappears after seven cycles, whereas the characteristic band with a marked vibrational fine structure from an aryl compound is observed at 250–270 nm, which is apparently assigned to ligand **a**. This indicates the variation of interaction between ligand **a** and rhodium catalyst, which might result from the formation of zero-valent rhodium colloids. In addition, the intensity variation of the absorbing tails in the visible region during recycling (see inset of Fig. 2) seems to be due to the scattering of the different size colloidal particles. Firstly the absorption intensity increases with developing runs and then starts to decrease after five cycles, indicating the growth of colloidal particles in the early cycles and size reduction in the post-cycles, which is in good agreement with the observations in TEM.

It is generally accepted that complexation of monophosphines gives rise to a weak ligand-to-metal bond strength. The rhodium carbonyl clusters $[Rh_4(CO)_{12}]$ and $[Rh_6(CO)_{16}]$, have been identified from infrared spectroscopy as the main

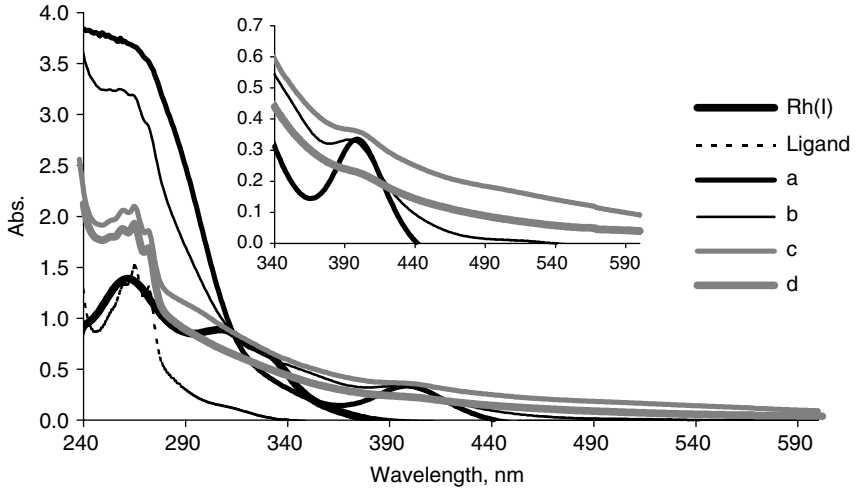

Figure 2. The UV–Vis spectra of the aqueous phase before and after reaction when using complex catalyst **A**: (a) before reaction; (b) first run; (c) fifth run; (d) seventh run. References: for Rh(I): $Rh(acac)(CO)_2$ in CH_2Cl_2; for ligand: ligand **a** in H_2O.

products in the hydroformylation post-reaction mixture when using [Rh(acac)(CO)(PPh_3)] as the catalyst.[40] Thus, in the present study the formation of Rh colloids via degradation of the above-mentioned Rh carbonyls is not surprising.

Leaching of catalytic material in the product phase is generally regarded as one key problem in recyclable catalytic systems.[41] Here, the product phase was examined by ICP-OES. After the first seven consecutive cycles, the amount of Rh metal leaching in the organic phase added up to 5.2%. However, increasing the ratio of 1-octene to catalyst ([Sub]/[Rh]) from 1000 (Table 1, entry 1) to 2000 (Table 1, entry 2) still gives rise to very high hydroformylation activity. Therefore, activity loss due to metal leaching can be ruled out in the present study. A further increase of [Sub]/[Rh] ratio to 4000 (Tabel 1, entry 3) leads to a relatively low aldehyde yield, while the isomeric octenes notably increase, which is comparable to the activity of the seventh cycle in entry 1. It is known that a catalyst concentration decrease in Rh/PPh_3 systems results in a lower selectivity in aldehydes and regioselectivity in the linear isomeric products.[42] With respect to entry 1, the colloidal precipitates would result in a low catalyst concentration in the reaction. Thus the hydroformylation activity loss shown in entry 1 might be due to the decreasing catalyst concentration in the aqueous phase. To prove this postulation, the activities of the rhodium colloids and agglomeration generated during the reaction have to be examined.

Colloidal catalyst B: Rh hydrosol 1/ligand a

Transition-metal colloids generally show poor catalytic activity in homogeneous catalysis due to decomposition or agglomeration processes in solution. To overcome this problem metal sols are immobilized on supports such as silica, charcoal, alumina or oxides.[43] Recently, immobilization of colloids in the aqueous phase based on biphasic catalysis has attracted growing attention.[8,44–47] In particular, numerous authors in the literature have reported the application of Rh colloidal catalysts in aqueous biphasic hydrogenation reactions.[3,44,45,47–49] However, biphasic hydroformylation reactions so far have been predominantly exemplified with homogeneous catalysts: Liu *et al*., however, reported hydroformylation of propylene with poly(*N*-vinyl-2-pyrrolidone)-protected Rh colloid in an aqueous biphasic system.[50]

Therefore, we decided to investigate the activity of colloidal Rh catalysts towards biphasic hydroformylation of 1-octene in the TRPTC system. At temperatures above the cloud point of ligand **a**, to some extent, Rh colloids might be transferred from aqueous phase into the organic phase.

Sulfobetaine-stabilized Rh(0) hydrosol **1** was prepared via Bönnemann's method using a THF-soluble 1 : 1 adduct of SB12 and Li[BEt_3H] as the reducing agent.[32,51] Transmission electron microscopy shows that the average particle size of colloid **1** is ~2.6 nm (see Fig. 3a). Because colloid **1** is water soluble, and a ligand exchange process by using ligand **a** to displace the original protecting shell (SB12)

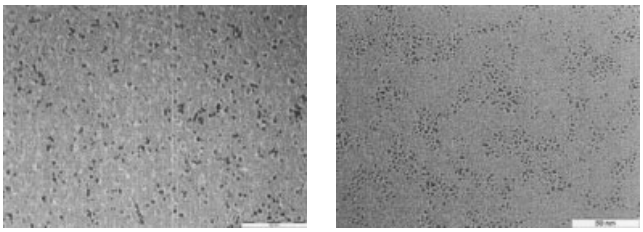

Figure 3. Transmission electron micrographs of Rh colloids: (a) **1** (2.6 ± 0.6 nm); (b) **2** (1.9 ± 0.4 nm). Scale bar: 50 nm.

Table 2. Hydroformylation[a] of 1-octene with colloidal catalyst **B** in the aqueous biphasic system

Cycle	Conversion (%)	S_{ald}[b] (%)	L/B ratio	S_{iso}[b] (%)
1	2.7	2.6	3.3	0.1
2	2.9	2.9	3.1	—

[a] Reaction conditions: $P_{initial} = 40$ bar (25 °C), $CO/H_2 = 1:1$, $T = 90$ °C, $t = 4$ h, $V_{organic}/V_{aqueous} = 1.5$, [Rh] = 3.6 mM, [P]/[Rh] = 5.
[b] S_{ald}, selectivity in aldehydes; S_{iso}, selectivity in isomeric octenes (2- and 3-octene).

Table 3. Hydroformylation[a] of 1-octene with complex catalyst **C** in the aqueous biphasic system

Cycle	Conversion (%)	S_{ald}[b] (%)	L/B ratio	S_{iso}[b] (%)
1	3.8	1.8	3.2	2.0
2	3.0	1.5	3.0	1.5

[a] Reaction conditions: $P_{initial} = 40$ bar (25 °C), $CO/H_2 = 1:1$, $T = 90$ °C, $t = 4$ h, $V_{organic}/V_{aqueous} = 1.5$, [Rh] = 3.6 mM, [P]/[Rh] = 5.
[b] S_{ald}, selectivity in aldehydes; S_{iso}, selectivity in isomeric octenes (2- and 3-octene).

seems unattainable, we introduced ligand **a** to an aqueous solution of colloid **1** with a ratio of [P]/[Rh] = 5 and then applied it to biphasic hydroformylation of 1-octene. The reaction was performed under identical conditions as using complex catalyst **A**. As shown in Table 2, colloidal catalyst **B** exhibits very low conversion rates. This result is apparently not comparable with that of catalyst **A**, considering that the activity of the latter is still very high after the colloidal formation. Furthermore, catalyst **C** prepared from $Rh(acac)(CO)_2$/TPPTS was also applied to the hydroformylation of 1-octene under identical conditions for the purpose of comparison. Table 3 presents the very low conversion rates when using catalyst **C**, which are related to the low solubility of 1-octene in the aqueous catalyst phase.[25] It can be concluded that colloidal catalyst **B** shows comparable hydroformylation activity to catalyst **C**. Therefore, the suspected thermomorphic behaviour of colloidal catalyst **B** might be suppressed completely due to the existence of the hydrophilic protecting shell (SB12) on colloidal surfaces. Consequently, the ligand

exchange process was tried by using a Rh organosol to obtain a 'clean' Rh(0) colloidal catalyst stabilized by ligand **a**.

Colloidal catalyst D: Rh organosol 2/ligand a

Bönnemann *et al*. have developed a general route to synthesize the transition-metal colloids in groups 6–11 by reducing the metal salts with tetraalkyl ammonium triorganohydroborates in THF.[52–58] It was suggested that the NR_4^+ salts were formed in high local concentration at the reduction centre as an efficient ligand shell to provide the colloids with redispersibility in organic solvents and prevent their aggregation.[55,56]

In this part, Rh organosol **2** was prepared according to Bönnemann's method (see Fig. 3b), and then the ammonium moieties on rhodium surfaces were displaced by ligand **a** to functionalize and immobilize the zero-valent Rh colloid in aqueous phase. The ligand exchange proceeds smoothly and a ligand-to-rhodium ratio of 5 is enough to disperse the Rh colloid in the aqueous phase. Monitoring the process via ^{1}H, ^{13}C and ^{31}P NMR revealed that ligand **a** in the toluene phase and $N(octyl)_4Cl$ in the water phase are almost not detectable. Thus a 'clean' colloidal Rh catalyst stabilized by ligand **a** has been obtained. The aqueous colloidal Rh solution is stable over months.

As shown in Table 4, the colloidal Rh catalyst **D** exhibits very high activity towards hydroformylation of 1-octene. The first cycle gives an aldehyde yield of 97.1% and an L/B ratio of 2.4, which is surprisingly identical to that using complex Rh(I) catalyst **A**. Similar to **A**, the hydroformylation activity decreases after recycling twice, along with increasing isomeric products from 1-octene.

Table 4. Hydroformylation[a] of 1-octene with colloidal catalyst **D** in the aqueous biphasic system

Entry	Cycle	Conversion (%)	S_{ald}[b] (%)	L/B ratio	S_{iso}[b] (%)
1[c]	1	99.8	97.1	2.4	2.7
	2	99.9	97.6	2.3	2.3
	3	99.6	94.2	2.3	5.4
	4	99.9	89.6	2.3	10.3
	5	99.8	81.7	2.3	18.1
	6	99.8	77.1	2.0	22.7
	7[d]	99.8	63.3	2.2	36.5
2[e]	1	96.7	74.6	1.5	22.1
3[f]	1	93.7	38.3	2.4	55.4
4[g]	1	99.7	85.4	1.4	14.3

[a] Reaction conditions: $P_{initial} = 40$ bar (25 °C), $CO/H_2 = 1:1$, $T = 90$ °C, $t = 4$ h, $V_{organic}/V_{aqueous} = 1.5$, [P]/[Rh] = 5.
[b] S_{ald}, selectivity in aldehydes; S_{iso}, selectivity in isomeric octenes (2- and 3-octene).
[c] [Rh] = 3.6 mM, ratio of 1-octene to catalyst ([Sub]/[Rh]) = 1000.
[d] Mercury poisoning experiments.
[e] [Rh] = 1.8 mM, [Sub]/[Rh] = 2000.
[f] [Rh] = 0.9 mM, [Sub]/[Rh] = 4000.
[g] [Rh] = 3.6 mM, [Sub]/[Rh] = 1000, [P]/[Rh] = 2.5.

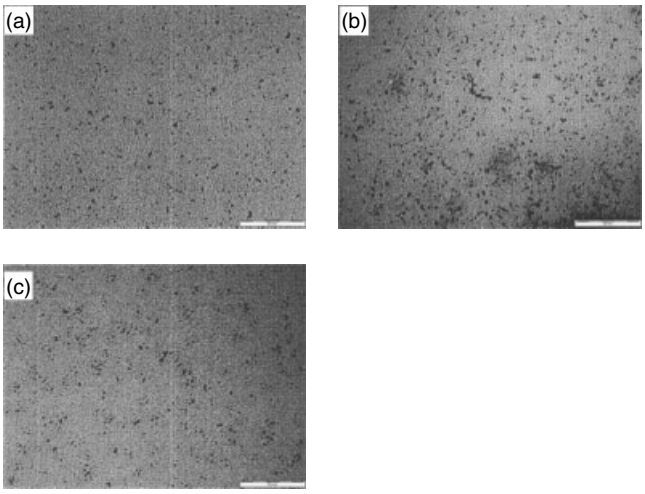

Figure 4. Transmission electron micrographs of the post-reaction aqueous phase when using colloidal catalyst **D**: (a) first run (2.3 ± 0.5 nm); (b) second run (2.0 ± 0.5 nm); (c) fourth run (1.8 ± 0.5 nm). Scale bar: 50 nm.

A TEM investigation of the aqueous phase (see Fig. 4) shows that the average particle size of Rh colloids increased from 1.9 nm originally to 2.3 nm after the first cycle. Then the average particle size decreases to 2.0 nm after the second cycle due to slight agglomeration, and to 1.8 nm after the fourth cycle. During the recycling steps, the colour of the aqueous phase changed from black–brown to light brown, indicating that agglomeration and precipitation of colloidal particles had occurred. After reaction, Rh black was found in the autoclave. These observations suggest that large Rh nanoparticles tend to aggregate very quickly under the hydroformylation reaction conditions, leading to immediate precipitation, in contrast to the observations made by TEM in the post-reaction aqueous phase.

The hydroformylation reaction also was performed at lower catalyst concentrations by increasing the ratio of [Sub]/[Rh] from 1000 (Table 4, entry 1) to 2000 and 4000 (Table 4, entries 2 and 3), respectively. A similar trend is observed with complex catalyst **A**, where the isomerization of 1-octene increases greatly with decreasing catalyst concentration. Inductively coupled plasma OES showed that the total amount of leaching rhodium in the organic phase of entry 1 was 3.4% after six cycles, these findings imply that the significant increase of isomeric octenes and decrease of hydroformylation activity after five cycles (Table 4, entry 1) result from the decreased rhodium concentrations in the biphasic system, which is attributed mainly to the agglomeration of colloidal Rh during repeated recycling.

The aqueous catalyst dispersions were examined also by UV–Vis spectroscopy before and after hydroformylation reactions. As shown in Fig. 5a, colloidal Rh catalyst **D** prepared from Rh organosol **2** and ligand **a** gives a characteristic absorption band arising from ligand **a** and

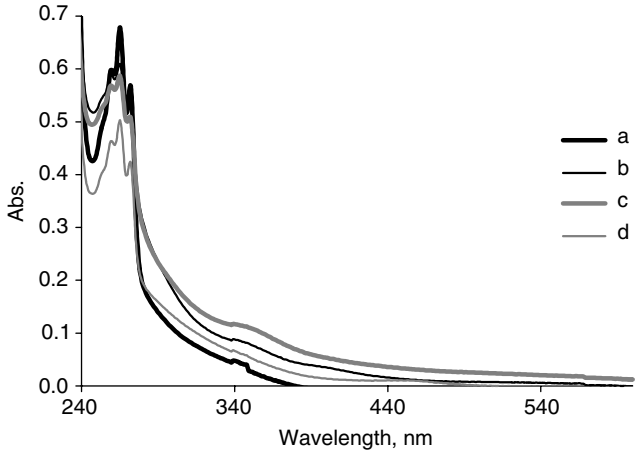

Figure 5. The UV–Vis spectra of the aqueous phase before and after reaction when using colloidal catalyst **D**: (a) before reaction; (b) first run; (c) second run; (d) fifth run.

a broad tailing absorption. No significant spectral changes were observed during recycling, except that the intensity of the broad tailing absorption underwent a similar fluctuation as observed in Fig. 1, due to the variation of Rh particle size.

To evaluate the contribution of the precipitates formed during recycling, mercury poisoning experiments were performed after six cycles (Table 4, entry 1). Mercury(0) is a well-known poison for heterogeneous catalysts due to its adsorption on the catalyst surface or amalgamation with the metal catalyst.[17,59,60] Because Rh metal does not form amalgams with Hg(0), large excess equivalents of Hg(0) (Hg(0)/Rh $\geq$ 300) have to be used to contact the catalyst surface sufficiently.[61] Here, 350 equivalents of Hg(0) were added into the aqueous catalyst phase and stirred at 25 °C for 1 h before performing the seventh cycle. From the results of the seventh cycle in entry 1 (Table 4), it seems that Hg(0) almost has no influence on reuse of the catalyst phase, indicating that the Rh precipitates formed during the reaction are not catalytically active. Therefore, the increasing isomerization during recycling can be attributed only to the low catalyst concentration in solution.

The above results suggest that the colloial Rh catalyst **D** stabilized by ligand **a** also demonstrates thermomorphic behaviour in the aqueous biphasic hydroformylation reaction. During recycling, colloidal agglomeration occurs and this results in the low catalyst concentration in the aqueous phase, which enhances the competing isomerization reaction and leads to a low hydroformylation activity.

However, because the complex Rh(I) catalyst **A** and the colloidal Rh(0) catalyst **D** exhibit identical catalytic activity, and determining the reaction mechanism in metal cluster catalysis is inherently difficult,[62] we cannot conclude on the 'true' active site during the early cycles of the TRPTC biphasic system. More work is necessary to resolve the 'precise nature' of the active species in colloidal metal catalysis.

It should be noted that we do not refer to ligand leaching because no significant changes of regioselectivity in linear aldehydes are observed, especially in the early cycles. As shown in Table 4 (entry 4), a remarkable decrease of the L/B ratio occurs when [P]/[Rh] = 2.5 is used. Thus, ligand leaching does not account for the observed catalytic deactivation.

CONCLUSION

The *in situ* formation of Rh colloids was observed when a TRPT complex Rh(I) catalyst **A** was applied to aqueous biphasic hydroformylation of 1-octene. These colloidal Rh particles show Ostwald ripening behaviour during recycling, and finally precipitate from the catalyst dispersion after long reaction times. This leads to a low catalyst concentration in the aqueous phase. As a consequence, the competing isomerization reaction rate is enhanced and the hydroformylation rates decrease. Furthermore, colloidal Rh catalyst **D** prepared from Rh organosol **2** and TRPT ligand **a** also exhibits a high activity in the hydroformylation of 1-octene, comparable to catalyst **A**. Although the thermomorphic behaviour accounts for its high activity in the biphasic system, Ostwald ripening and activity decay of colloidal Rh catalyst **D** are also observed. These findings suggest that the *in situ*-generated colloids (2.2 nm) in the classic TRPT complex Rh(I) catalytic system do not deactivate the hydroformylation activity during the first steps of recycling. However, they are liable to agglomeration after long reaction times and finally precipitate. This leads to low catalyst concentrations in the biphasic system and subsequently to the 'death' of Rh catalyst.

Attempts should be made to prevent Rh colloidal growth and increase the stability of TRPT complex Rh(I) catalysts, by using bidentate phosphine ligands with distinct cloud points. This work implies that colloidal Rh catalysts stabilized by TRPT ligands demonstrate thermomorphic behaviour in an aqueous biphasic reaction. Bönnemann's method, particularly using colloid **2** stabilized by TRPT ligands, has great potential to widen the scope of colloidal catalyst applications in biphasic catalytic reactions under mild conditions.

Acknowledgements

The authors would like to thank the gas chromatography, mass spectroscopy and electron microscopy groups in the Max-Planck-Institut für Kohlenforschung for the measurements and characterization of the samples.

REFERENCES

1. Schmid G. *Chem. Rev.* 1992; **92**: 1709.
2. Pellegatta JL, Blandy C, Choukroun R, Lorber C, Chaudret B, Lecante P, Snoeck E. *New. J. Chem.* 2003; **27**: 1528.
3. Borsla A, Wilhelm AM, Delmas H, *Catal. Today* 2001; **66**: 389.

4. Bronstein LM, Chernyshov DM, Volkov IO, Ezernitskaya MG, Valetsky PM, Matveeva VG, Sulman EM. *J. Catal.* 2000; **196**: 302.
5. Bönnemann H, Richards RM. *Eur. J. Inorg. Chem.* 2001; **10**: 2455.
6. Bönnemann H, Nagabhushana KS. In *Encyclopedia of Nanoscience and Nanotechnology*, Nalwa HS (ed.), vol. 1. American Scientific Publishers: California, 2004; 777–813.
7. Bönnemann H, Richards RM. In *Synthetic Methods of Organometallic and Inorganic Chemistry*, Herrmann WA (ed.), vol. 10, Thieme Medical Publishers: New York, 2002; 209–224.
8. Launay F, Roucoux A, Patin H. *Tetrahedron Lett.* 1998; **39**: 1353.
9. Duff DG, Baiker A. *Stud. Surf. Sci. Catal.* 1995; **91**: 505.
10. Vargaftik MN, Zagorodnikov VP, Stolarov IP, Moiseev II, Kochubey DI, Likholobov VA, Chuvilin AL, Zamaraev KI. *J. Mol. Catal.* 1989; **53**: 315.
11. Chauhan M, Hauck BJ, Keller LP, Boudjouk P. *J. Organomet. Chem.* 2002; **645**: 1.
12. Schmid G, West H, Mehles H, Lehnert A. *Inorg. Chem.* 1997; **36**: 891.
13. Lewis LN, Lewis N, Uriarte RJ. *Adv. Chem. Ser.* 1992; 541.
14. Stein J, Lewis LN, Gao Y, Scott RA. *J. Am. Chem. Soc.* 1999; **121**: 3693.
15. Reetz MT, Westermann E. *Angew. Chem. Int. Ed.* 2000; **39**: 165.
16. Le Bars J, Specht U, Bradley JS, Blackmond DG. *Langmuir* 1999; **15**: 7621.
17. Widegren JA, Finke RG. *J. Mol. Catal. A—Chem.* 2003; **198**: 317.
18. Reetz MT, de Vries JG. *Chem. Commun.* 2004; 1559.
19. Na Y, Park S, Han SB, Han H, Ko S, Chang S. *J. Am. Chem. Soc.* 2004; **126**: 250.
20. Chauhan BPS, Rathore JS, Chauhan M, Krawicz A. *J. Am. Chem. Soc.* 2003; **125**: 2876.
21. Widegren JA, Bennett MA, Finke RG. *J. Am. Chem. Soc.* 2003; **125**: 10 301.
22. Dissanayake DP, Lunsford JH. *J. Catal.* 2003; **214**: 113.
23. Temple K, Jakle F, Sheridan JB, Manners I. *J. Am. Chem. Soc.* 2001; **123**: 1355.
24. Cornils B, Wiebus E. *Chemtech* 1995; **25**: 33.
25. Lipps W, Bahrmann H, Cornils B, Konkol W. Patent, DE3420491, 1985.
26. Bahrmann H, Bogdanovic S, Van Leeuwen PWNM. In *Aqueous-Phase Organometallic Catalysis: Concepts and Applications*, (2nd edn), Cornils B, Herrmann WA (eds). Wiley-VCH: Weinheim, 2004; 391–409.
27. Jin ZL, Zheng XL, Fell B. *J. Mol. Catal. A—Chem.* 1997; **116**: 55.
28. Jin ZL, Yan YY, Zuo HP, Fell B. *J. Prak. Chem.-Chem. Ztg.* 1996; **338**: 124.
29. Wang YH, Jiang JY, Jin ZL. *Catal. Surv. Asia* 2004; **8**: 119.
30. Jin ZL, Wang YH, Zheng XL. In *Aqueous-Phase Organometallic Catalysis: Concepts and Applications*, (2nd edn), Cornils B, Herrmann WA (eds). Wiley-VCH: Weinheim, 2004; 301–312.
31. Zheng XL, Jiang JY, Liu XZ, Jin ZL. *Catal. Today* 1998; **44**: 175.
32. Bönnemann H, Brijoux W. In *Advanced Catalysts and Nanostructured Materials: Modern Synthetic Methods*, Moser WR (ed.). Academic Press: 1996; 165–196.
33. Bönnemann H, Brijoux W, Brinkmann R, Dinjus E, Joussen T, Korall B. *Angew. Chem. Int. Ed.* 1991; **30**: 1312.
34. Marko IE, Sterin S, Buisine O, Mignani R, Branlard P, Tinant B, Declercq JP. *Science* 2002; **298**: 204.
35. Narayanan R, El-Sayed MA. *J. Am. Chem. Soc.* 2003; **125**: 8340.
36. Howard A, Mitchell CEJ, Egdell RG. *Surf. Sci.* 2002; **515**: L504.
37. Imre A, Beke DL, Gontier-Moya E, Szabo IA, Gillet E. *Appl. Phys. A—Mater.* 2000; **71**: 19.
38. Jain SC, Hughes AE. *J. Mater. Sci.* 1978; **13**: 1611.
39. Creighton JA, Eadon DG. *J. Chem. Soc. Faraday Trans.* 1991; **87**: 3881.
40. Mieczynska E, Trzeciak AM, Ziolkowski JJ. *J. Mol. Catal.* 1992; **73**: 1.
41. Herrmann WA, Cornils B. *Angew. Chem. Int. Ed.* 1997; **36**: 1049.
42. Brown CK, Wilkinson G. *J. Chem. Soc. A* 1970; 2753.
43. Roucoux A, Schulz J, Patin H. *Chem. Rev.* 2002; **102**: 3757.
44. Roucoux A, Schulz J, Patin H. *Adv. Synth. Catal.* 2003; **345**: 222.
45. Schulz E, Levigne S, Roucoux A, Patin H. *Adv. Synth. Catal.* 2002; **344**: 266.
46. Bhanage BM, Arai M. *Catal. Rev.* 2001; **43**: 315.
47. Schulz J, Roucoux A, Patin H. *Chem.-Eur. J.* 2000; **6**: 618.
48. Pellegatta JL, Blandy C, Colliere V, Choukroun R, Chaudret B, Cheng P, Philippot K. *J. Mol. Catal. A—Chem.* 2002; **178**: 55.
49. Larpent C, Menn FBL, Patin H. *New J. Chem.* 1991; **15**: 361.
50. Han M, Liu HF. *Macromol. Symp.* 1996; **105**: 179.
51. Rothe J, Pollmann J, Franke R, Hormes J, Bönnemann H, Brijoux W, Siepen K, Richter J. *Fresenius J. Anal. Chem.* 1996; **355**: 372.
52. Bönnemann H, Braun G, Brijoux W, Brinkmann R, Tilling AS, Seevogel K, Siepen K. *J. Organomet. Chem.* 1996; **520**: 143.
53. Bönnemann H, Brijoux W. In *Active Metals: Preparation Characterization Applications*, Fürstner A (ed.). VCH Weinheim: New York, 1996; 339–379.
54. Bönnemann H, Brijoux W, Brinkmann R, Fretzen R, Joussen T, Köppler R, Korall B, Neiteler P, Richter J. *J. Mol. Catal.* 1994; **86**: 129.
55. Bönnemann H, Brinkmann R, Neiteler P. *Appl. Organomet. Chem.* 1994; **8**: 361.
56. Bucher S, Hormes J, Modrow H, Brinkmann, R, Waldofner N, Bönnemann H, Beuermann L, Krischok S, Maus-Friedrichs W, Kempter V. *Surf. Sci.* 2002; **497**: 321.
57. Bönnemann H, Brinkmann R, Köppler R, Neiteler P, Richter J. *Adv. Mater.* 1992; **4**: 804.
58. Bönnemann H, Brijoux W, Brinkmann R, Dinjus E, Fretzen R, Joussen T, Korall B. *J. Mol. Catal.* 1992; **74**: 323.
59. Whitesides GM, Hackett M, Brainard RL, Lavalleye JPPM, Sowinski AF, Izumi AN, Moore SS, Brown DW, Staudt EM. *Organometallics* 1985; **4**: 1819.
60. Georgiades GC, Sermon PA. *J. Chem. Soc. Chem. Commun.* 1985; 975.
61. Weddle KS, Aiken JD, Finke RG. *J. Am. Chem. Soc.* 1998; **120**: 5653.
62. Puddephatt RJ. In *Metal Clusters in Chemistry*; Braunstein P, Oro LA, Raithby PR (eds), vol. 2, Wiley-VCH: Weinheim, 1999; 605–615.
63. Solinas M. PhD Thesis, RWTH, Aachen, 2004.